

# On possibility of time reversal symmetry violation in neutrino elastic scattering on polarized electron target

W. Sobków<sup>a,1</sup>, A. Błaut<sup>b,1</sup>

<sup>1</sup> Institute of Theoretical Physics, University of Wrocław, Pl. M. Born 9, PL-50-204 Wrocław, Poland

Received: date / Accepted: date

**Abstract** In this paper, we indicate a possibility of utilizing the elastic scattering of the Dirac low energy ( $\sim 1$  MeV) electron neutrinos ( $\nu_e$ 's) on the polarized electron target (PET) in testing the time reversal symmetry violation (TRSV). We consider a scenario in which the incoming  $\nu_e$  beam is the superposition of left chiral (LC) and right chiral (RC) states. LC  $\nu_e$ 's interact mainly by the standard  $V - A$  and small admixture of non-standard scalar  $S_L$ , pseudoscalar  $P_L$ , tensor  $T_L$  interactions, while RC ones are only detected by the exotic  $V + A$  and  $S_R, P_R, T_R$  interactions. In addition, one assumes that the spin polarization vector of the initial  $\nu_e$ 's is turned aside from its momentum, and due to this the non-vanishing transversal component of the  $\nu_e$  spin polarization appears. We compute the differential cross section as a function of the recoil electron azimuthal angle and scattered electron energy, and show how the interference terms between standard  $V - A$  and exotic  $S_R, P_R, T_R$  couplings depend on the various angular correlations among the transversal  $\nu_e$  spin polarization, the polarization of the electron target, the incoming neutrino momentum and the outgoing electron momentum in the limit of relativistic  $\nu_e$ . We illustrate how the maximal value of recoil electrons azimuthal asymmetry and the asymmetry axis location of outgoing electrons depend on the azimuthal angle of the transversal component of the  $\nu_e$  spin polarization, both for the time reversal symmetry conservation (TRSC) and TRSV. Next, we display that the electron energy spectrum and polar angle distribution of the recoil electrons are also sensitive to the interference terms between  $V - A$  and  $S_R, P_R, T_R$  couplings, proportional to the T-even and T-odd angular correlations among the transversal  $\nu_e$  polarization, the electron polarization of the target, and the incoming  $\nu_e$  momentum, respectively. Our model-independent analysis is carried out for the flavor  $\nu_e$ 's. To

make such tests feasible, the intense (polarized) artificial  $\nu_e$  source, PET and the appropriate detector measuring the directionality of the outgoing electrons, and/or the recoil electrons energy with a high resolution have to be identified.

## 1 Introduction

One of the fundamental problems in the neutrino physics is whether TRSV takes place in purely leptonic processes at low energies (e. g. the neutrino-electron elastic scattering (NEES)). According to the standard electro-weak model (SM) [1–5], the V and A couplings of LC  $\nu_e$ 's may only participate in NEES and the hermiticity conditions of interaction lagrangian require the real coupling constants. This means that there is no possibility of appearing TRSV correlations in the differential cross section for the NEES, even when the electron target is polarized. The qualitative change emerges when the exotic scalar (S), tensor (T), pseudoscalar (P) and (V+A) couplings of the interacting RC  $\nu$ 's beyond the SM in addition to the standard V-A ones are introduced. The presence of the exotic complex couplings together with PET may generate the non-vanishing T-even and T-odd angular correlations in the differential cross section. It is worth pointing out that the TRSV (equivalent CP violation in the case of CPT-invariant theory) is observed in the decays of neutral kaons and B-mesons [6–8], and described by a single phase of the Cabibbo-Kobayashi-Maskawa quark-mixing matrix (CKM) [9]. However, this CP-violating phase does not allow for explanation of the existing matter-antimatter asymmetry of universe and new T-violating phases are needed [10]. It is important to note that the available experimental results still do not rule out the scenarios with the exotic S, T, P and V+A weak interactions of RC  $\nu$ 's. The various non-standard gauge models including exotic TRSV interactions, RC  $\nu$ 's, mechanisms explaining the origin of parity viola-

<sup>a</sup>e-mail: wieslaw.sobkow@ift.uni.wroc.pl

<sup>b</sup>e-mail: arkadiusz.blaut@ift.uni.wroc.pl

tion and of fermion generations, masses, mixing and smallness of  $\nu$  mass have been proposed. We mean, e. g., the left-right symmetric models (LRSM) [11–15], composite models [16–18], models with extra dimensions (MED) [19] and the unparticle models (UP) [20–32]. Concerning the UP theory, it is noteworthy that in this scheme  $\nu$ 's with the different chiralities can interact with the spin-0 scalar, spin-1 vector, spin-2 tensor unparticle sectors and consequently one gets the amplitudes for the low energy leptonic processes in the form of unparticle four-fermion contact interaction with the non-standard S, T, P, V+A lorentz interactions.

In spite of experimental limitations and lack of unambiguous indication of the non-standard model, there is a constant necessity of increase of the precision of present tests at low energies, and on the other hand, it seems sensible to search for new tools sensitive to the linear effects from the exotic complex couplings of RC  $\nu$ 's, because the measurements of these observables may shed some new light on the TRSV in the leptonic interactions. As it is known the future super-beam and neutrino factory projects aim at the tests of the CP violation in the lepton sector, where simultaneously  $\nu$  and  $\bar{\nu}$  oscillations would be measured [33, 34]. Also other proposals of observables for the tests on the TRSV in the leptonic and semileptonic processes: the precise measurements of T-odd triple-correlations for the massive charged leptons [35–39], of electric dipole moments of the neutron and atoms are worth noticing [40–44]. Till now, all the evidence is consistent with the TRSC scenario.

Our considerations show that NEES on PET offers new scientific opportunities for the studies on the TRSV in the leptonic reactions. From the perspective of the main goals of this paper, it is essential to mention the recent tests confirming the possibility of realizing the polarized target crystal of  $Gd_2SiO_5$  doped with Cesium [45], as suggested in [46]. The concepts of using PET to probe the neutrino magnetic moments, the flavor composition of (anti)neutrino beam, axions, spin-spin interaction in gravitation [47–54] are also worth noting.

In this study, we focus on the elastic scattering of low energy Dirac  $\nu_e$ 's on PET. We show in a model-independent way how the admixture of the exotic S, T, P, V+A complex couplings of RC  $\nu_e$ 's in addition to the standard V, A real couplings of LC ones affects on the azimuthal distribution and asymmetry of the recoil electrons, polar distribution of scattered electrons and their energy spectrum, and consequently on the possibility of TRSV in the relativistic  $\nu_e$  limit. Our studies are made for the flavor-eigenstate (current) Dirac  $\nu_e$ 's and when the monochromatic  $\nu_e$  source is deployed at a near distance from the detector. We analyze the various scenarios assuming that the hypothetical detector is able to measure both the azimuthal angle  $\phi_e$  and polar angle  $\theta_e$  of the recoil electrons, and/or also the energy of the outgoing electrons with a high resolution. In order to com-

pute the expected effects, we use the experimental values of standard couplings:  $c_V^L = 1 + (-0.04 \pm 0.015)$ ,  $c_A^L = 1 + (-0.507 \pm 0.014)$  [55].

## 2 Elastic scattering of Dirac electron neutrinos on polarized electrons - basic assumptions

We assume that the incoming Dirac  $\nu_e$  beam is generated by the monochromatic low energy ( $\sim 1MeV$ ) and polarized source ( $\nu_e$  emitter with a high intensity). Let us remind that the  $^{51}Cr$  unpolarized emitter with a high activity  $\sim 370 PBq$  in the SOX experiment [56] (Short distance Oscillation with boreXino) at the Borexino detector is planed to search for among other the sterile  $\nu_e$ 's [57–63]. Moreover, one supposes that the initial  $\nu_e$  flux is the superposition of LC states detected mainly by the standard  $V - A$  and small admixture of non-standard scalar  $S_L$ , pseudoscalar  $P_L$ , tensor  $T_L$  interactions, while RC ones interact only by the exotic  $V + A$  and  $S_R, P_R, T_R$  interactions. Additionally, one admits that the initial  $\nu_e$  beam has the spin polarization vector turned aside from its momentum, and in this way the non-vanishing transversal components of the spin polarization appear. In order to illustrate the possibility of producing the  $\nu_e$  beam with the non-zero transversal spin polarization, we refer to the ref. [64], where the muon capture by proton as the production process of L-R chiral superposition has been considered. In the next studies, the other sources are going to be analyzed. It should be stressed that when the admixture of RC  $\nu$ 's in addition to the LC ones in the polarized  $\nu$  source is admitted and the production plane is assigned, the  $\nu$  spin polarization vector may acquire the transversal components, potentially giving both T-even and T-odd effects. These transversal  $\nu$  polarizations consist only of the interferences between the  $(V, A)_L$  and  $(S, T, P)_R$  couplings and do not vanish in the relativistic  $\nu$  limit. We have completely different situation for the longitudinal  $\nu$  polarization, where all the interferences between the  $V - A$  and  $(S, T, P)_R$  interactions are strongly suppressed by  $\nu$  mass. It means that only the squares of exotic RC couplings (at most the interferences within exotic couplings) and of standard LC ones may generate the possible effect. The amplitude for the  $\nu_e e^-$  scattering takes the form:

$$\begin{aligned}
M_{\nu_e e^-}^D = \frac{G_F}{\sqrt{2}} \{ & (\bar{u}_{e'} \gamma^\alpha (c_V^L - c_A^L \gamma_5) u_e) (\bar{u}_{\nu_e'} \gamma_\alpha (1 - \gamma_5) u_{\nu_e}) \\
& + (\bar{u}_{e'} \gamma^\alpha (c_V^R + c_A^R \gamma_5) u_e) (\bar{u}_{\nu_e'} \gamma_\alpha (1 + \gamma_5) u_{\nu_e}) \quad (1) \\
& + c_S^R (\bar{u}_{e'} u_e) (\bar{u}_{\nu_e'} (1 + \gamma_5) u_{\nu_e}) \\
& + c_P^R (\bar{u}_{e'} \gamma_5 u_e) (\bar{u}_{\nu_e'} \gamma_5 (1 + \gamma_5) u_{\nu_e}) \\
& + \frac{1}{2} c_T^R (\bar{u}_{e'} \sigma^{\alpha\beta} u_e) (\bar{u}_{\nu_e'} \sigma_{\alpha\beta} (1 + \gamma_5) u_{\nu_e}) \\
& + c_S^L (\bar{u}_{e'} u_e) (\bar{u}_{\nu_e'} (1 - \gamma_5) u_{\nu_e}) \\
& + c_P^L (\bar{u}_{e'} \gamma_5 u_e) (\bar{u}_{\nu_e'} \gamma_5 (1 - \gamma_5) u_{\nu_e})
\end{aligned}$$

$$+ \frac{1}{2} c_T^L (\bar{u}_{e'} \sigma^{\alpha\beta} u_e) (\bar{u}_{\nu_e'} \sigma_{\alpha\beta} (1 - \gamma_5) u_{\nu_e}),$$

where  $G_F = 1.1663788(7) \times 10^{-5} \text{GeV}^{-2} (0.6 \text{ ppm})$  [65] is the Fermi constant. The coupling constants are denoted with the superscripts  $L$  and  $R$  as  $c_V^{L,R}$ ,  $c_A^{L,R}$ ,  $c_S^{R,L}$ ,  $c_P^{R,L}$ ,  $c_T^{R,L}$  respectively to the incoming  $\nu_e$  of left- and right-handed chirality. Because we admit the TRSV, the non-standard coupling constants  $c_S^{R,L}$ ,  $c_P^{R,L}$ ,  $c_T^{R,L}$  are the complex numbers denoted as  $c_S^R = |c_S^R| e^{i\theta_{S,R}}$ ,  $c_S^L = |c_S^L| e^{i\theta_{S,L}}$ , etc. Moreover, the relations between the exotic couplings,  $c_{S,T,P}^L = c_{S,T,P}^{*R}$  appearing at the level of interaction lagrangian should be taken into account. It manifests the lack of dependence of the square terms coming from the  $S, T, P$  interactions in the cross section on the longitudinal  $\nu_e$  polarization  $\hat{\eta}_\nu \cdot \hat{\mathbf{q}}$ . The general formula for the differential cross section with the dependence on the azimuthal angle of outgoing electron momentum, when  $\hat{\eta}_e \perp \hat{\mathbf{q}}$ , is presented in the appendix. Calculations are carried out with the use of the covariant projectors for the incoming  $\nu_e$ 's (including both the longitudinal and transverse components of the spin polarization) in the relativistic limit and for the polarized target-electrons, respectively [66].

### 3 Azimuthal distribution and asymmetry of recoil electrons

In this section, we analyze the possibility of using the azimuthal distribution of recoil electrons for the investigation of TRSV in the  $\nu$  elastic scattering on PET. According to the SM, the mentioned azimuthal distribution has a local maximum at  $\Phi = \pi/2$  as it is illustrated in the Fig.2 and Fig.3, respectively. The Fig. 2 is the polar plot of  $d^2\sigma/d\phi_e d\theta_e = (d^2\sigma/d\phi_e dy) \cdot (dy/d\theta_e)$  as a function of  $\phi_e$  for the assigned values of  $\theta_e$ . The Fig. 3 is the polar plot of  $d^2\sigma/d\phi_e dy$  as a function of  $\phi_e$  for the assigned values of  $y$ . These two plots reveal the up-down azimuthal symmetry measured with respect to  $\Phi = 0$  and the left-right azimuthal asymmetry with the asymmetry axis directed along  $\Phi = \pi/2$ , clearly visible for  $d^2\sigma/d\phi_e d\theta_e$ . Moreover, it is important to stress that in the case of the standard  $V - A$  interaction, the asymmetry axis is fixed at  $\Phi = \pi/2$  and is independent of the variations of  $y$ ,  $\theta_e$ ,  $E_\nu$  and the standard  $c_V^L$ ,  $c_A^L$  couplings values but the degree of the asymmetry can change. Usually to quantify the azimuthal asymmetry one makes use of the asymmetry function (see Appendix 2 for the definitions). Fig.4 displays the maximal values of azimuthal asymmetries  $A_y(\Phi = \pi/2)$  and  $A_{\theta_e}(\Phi = \pi/2)$  as functions of  $y$  and  $\theta_e$  for the standard  $V - A$  interaction. In both cases the maximal values of the  $A_y$  and  $A_{\theta_e}$  are equal to 0.0794, and achieved at  $y^{max} \approx 0.5$  and  $\theta_e^{max} \approx \pi/6$ , respectively. In order to illustrate how the phase of given exotic coupling and the azimuthal angle of  $(\hat{\eta}_\nu)^\perp$  affect the azimuthal asymmetry of recoil electrons, and consequently to hint to the possibility of TRSV,

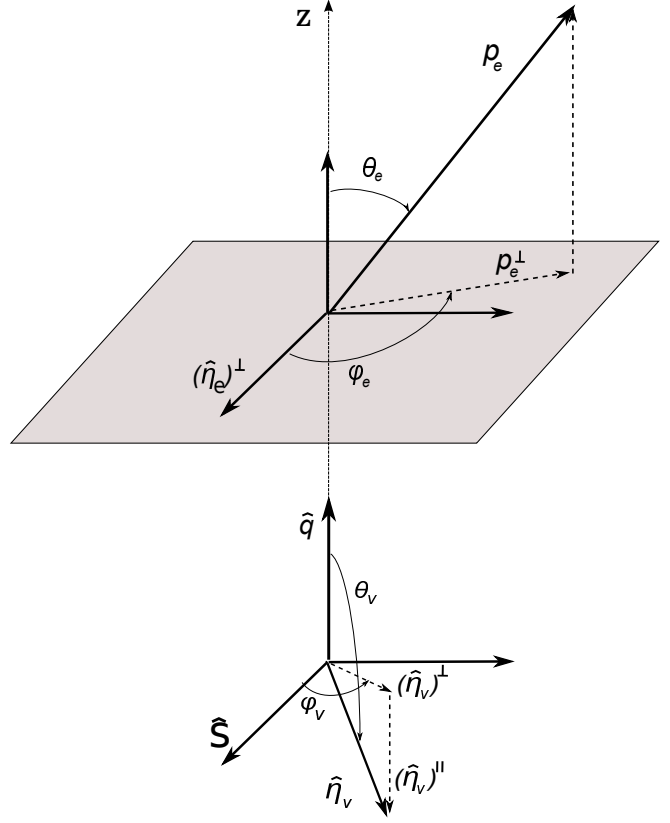


**Fig. 1** Production plane of the  $\nu_e$  beam is spanned by the polarization unit vector  $\hat{S}$  of source and the  $\nu_e$  LAB momentum unit vector  $\hat{\mathbf{q}}$ . Reaction plane is spanned by  $\hat{\mathbf{q}}$  and the transverse electron polarization vector of target  $(\hat{\eta}_e)^\perp$  (due to  $\hat{\eta}_e \perp \hat{\mathbf{q}}$ ) for  $\nu_e + e^- \rightarrow \nu_e + e^-$ .  $\theta_e$  is the polar angle between  $\hat{\mathbf{q}}$  and the unit vector  $\hat{\mathbf{p}}_e$  of recoil electron momentum.  $\phi_e$  is the angle between  $(\hat{\eta}_e)^\perp$  and the transversal component of outgoing electron momentum  $(\hat{\mathbf{p}}_e)^\perp$ .  $\hat{\eta}_\nu = (\sin \theta_\nu \cos \phi_\nu, \sin \theta_\nu \sin \phi_\nu, \cos \theta_\nu)$ .

we present the explicit form of the  $A(\Phi)$  asymmetry function for the scenario with  $V - A$  and  $S_R$  interactions:

$$A_{V-A}^{S,R}(\Phi) = 3\sqrt{m_e(2E_\nu + m_e)} \left[ -(c_A^L - c_V^L)(3c_A^L E_\nu + c_V^L E_\nu + 2c_A^L m_e) \sin^2 \frac{\theta_\nu}{2} \sin \Phi + |c_S^R| c_V^L (2E_\nu + m_e) \sin(\theta_{S,R} - \Phi + \phi_\nu) \right] / \left[ 4(|c_S^R|^2 + 4(c_A^{L2} + c_A^L c_V^L + c_V^{L2})) E_\nu^2 + 12(2c_A^{L2} + |c_S^R|^2 + c_A^L c_V^L + c_V^{L2}) E_\nu m_e + 3(3c_A^{L2} + 2|c_S^R|^2 + c_V^{L2}) m_e^2 - (4c_A^L c_V^L E_\nu (4E_\nu + 3m_e) + c_A^{L2} (4E_\nu + 3m_e)^2 + c_V^{L2} (16E_\nu^2 + 12E_\nu m_e + 3m_e^2)) \cos \theta_\nu - |c_S^R| (6(c_A^L + c_V^L) E_\nu^2 + (13c_A^L + 5c_V^L) E_\nu m_e + 6c_A^L m_e^2) \cos(\theta_{S,R} + \phi_\nu) \right]. \quad (2)$$

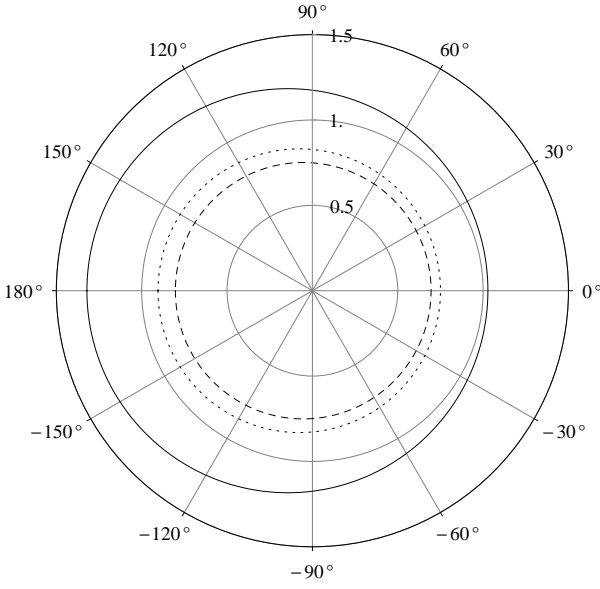


**Fig. 2** Dependence of  $d^2\sigma/d\phi_e d\theta_e$  on  $\phi_e$  for the standard V-A interaction,  $E_\nu = 1\text{ MeV}$ :  $\theta_e = \pi/12$  (dotted line),  $\theta_e = \pi/6$  (solid line),  $\theta_e = \pi/3$  (dashed line).

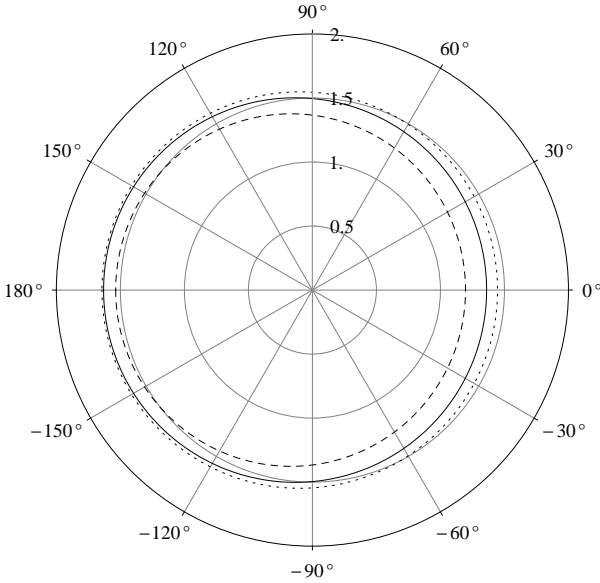


**Fig. 3** Dependence of  $d^2\sigma/d\phi_e dy$  on  $\phi_e$  for the standard V-A interaction,  $E_\nu = 1\text{ MeV}$ :  $y = 0.1$  (dotted line),  $y = 0.2$  (solid line),  $y = 0.5$  (dashed line).

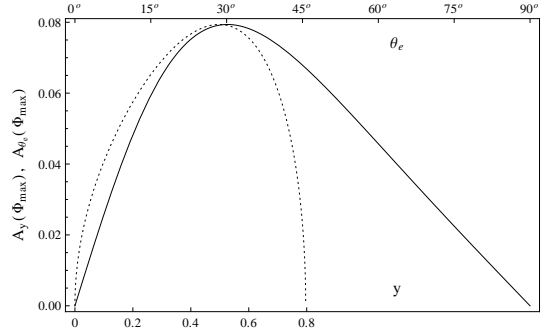


**Fig. 4** Standard V-A interaction,  $E_\nu = 1\text{ MeV}$ . Plot of the azimuthal asymmetry functions:  $A_y(\Phi = \pi/2)$  as a function  $y$  (solid line) and  $A_{\theta_e}(\Phi = \pi/2)$  as a function of  $\theta_e$  (dotted line).

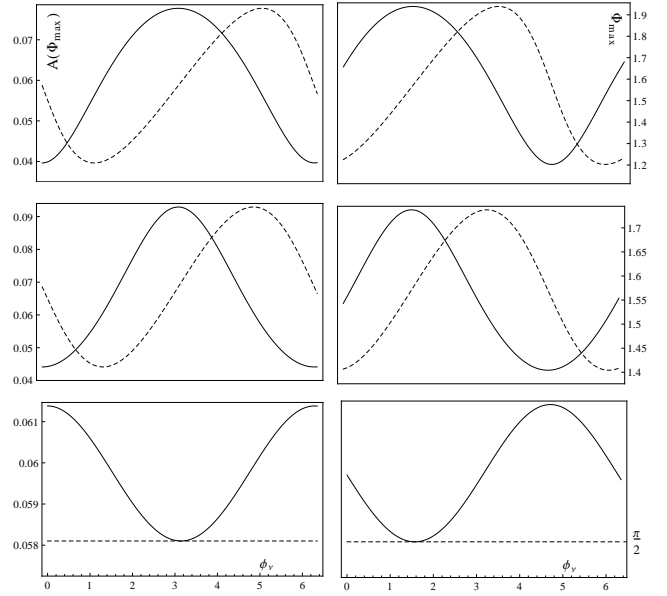


**Fig. 5** Dependence of  $A(\Phi_{max})$  on  $\phi_\nu$  (solid line) and  $\Phi_{max}$  on  $\phi_\nu$  (dashed line), for  $\hat{\eta}_\nu \cdot \hat{\mathbf{q}} = -0.95$ ,  $E_\nu = 1\text{ MeV}$ . TRSC: Upper left plot for the case of V-A and  $T_R$  when  $|c_T^R| = 0.2$ ,  $\theta_{T,R} = 0$ ; Middle left plot for the combination of V-A with  $S_R$  when  $|c_S^R| = 0.2$ ,  $\theta_{S,R} = 0$ ; Lower left plot for the case of V-A with  $P_R$  when  $|c_P^R| = 0.2$ ,  $\theta_{P,R} = 0$ . TRSV: Upper right plot for the scenario with V-A and  $T_R$  when  $|c_T^R| = 0.2$ ,  $\theta_{T,R} = \pi/2$ ; Middle right plot for the case of V-A and  $S_R$  when  $|c_S^R| = 0.2$ ,  $\theta_{S,R} = \pi/2$ ; Lower right plot for the combination of V-A with  $P_R$  when  $|c_P^R| = 0.2$ ,  $\theta_{P,R} = \pi/2$ .

We see that if  $|c_S^R| \sin(\theta_{S,R} + \phi_\nu) = 0$  then the local extremum of  $A_{V-A}^{S,R}(\Phi)$  is at  $\Phi = \pi/2$ . Assuming no  $T_R$  and  $P_R$  interactions it follows that any departure from the  $\Phi_{max} = \pi/2$  orientation of the asymmetry axis signals the presence of the exotic  $c_S^R$  interaction. Moreover, if the location of the asymmetry axis is sensitive to the relative orientation of PET and  $(\hat{\eta}_\nu)^\perp$  one can conclude that  $\theta_{S,R} + \phi_\nu \neq 0$ ; ideally, experimental control of  $\phi_\nu$  would give an opportunity to measure  $\theta_{S,R}$ . For example,  $\theta_{S,R}$  can be determined as  $-\phi_\nu$  for that value of  $\phi_\nu$  which fixes the asymmetry axis at the standard

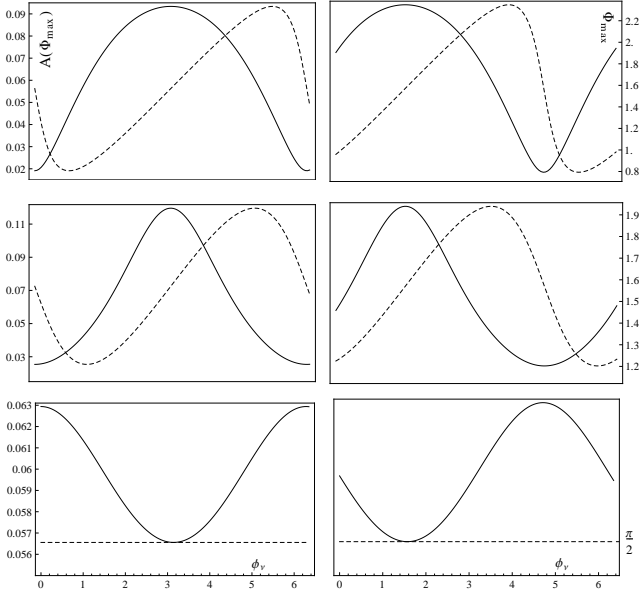


**Fig. 6** Dependence of  $A(\Phi_{max})$  on  $\phi_v$  (solid line) and  $\Phi_{max}$  on  $\phi_v$  (dashed line), for  $\theta_v = \pi/2$ ,  $E_v = 1 MeV$ . TRSC: Upper left plot for the case of  $V-A$  and  $T_R$  when  $|c_T^R| = 0.2$ ,  $\theta_{T,R} = 0$ ; Middle left plot for the combination of  $V-A$  with  $S_R$  when  $|c_S^R| = 0.2$ ,  $\theta_{S,R} = 0$ ; Lower left plot for the case of  $V-A$  with  $P_R$  when  $|c_P^R| = 0.2$ ,  $\theta_{P,R} = 0$ . TRSV: Upper right plot for the scenario with  $V-A$  and  $T_R$  when  $|c_T^R| = 0.2$ ,  $\theta_{T,R} = \pi/2$ ; Middle right plot for the case of  $V-A$  and  $S_R$  when  $|c_S^R| = 0.2$ ,  $\theta_{S,R} = \pi/2$ ; Lower right plot for the combination  $V-A$  with  $P_R$  when  $|c_P^R| = 0.2$ ,  $\theta_{P,R} = \pi/2$ .

$\pi/2$  location. The similar regularity holds for the case of  $V-A$  and  $T_R$  interactions, i.e. when  $|c_T^R| \sin(\theta_{T,R} + \phi_v) = 0$  then the local extremum of  $A_{V-A}^{T,R}(\Phi)$  must be at  $\Phi = \pi/2$ . For the variant with  $V-A$  and  $P_R$  couplings the situation is different: in this case  $\Phi_{max} = \pi/2$  independently of the coupling  $c_P^R$  and the azimuthal angle  $\phi_v$ .

The diagrams on Figs. 5, 6 show dependence of  $A(\Phi_{max})$  (solid lines) and  $\Phi_{max}$  (dashed lines) on  $\phi_v$  for the various scenarios with TRSC (left plots) and TRSV (right plots).

#### 4 Spectrum of recoil electrons and polar angle distribution of scattered electrons

In this section, we indicate the usefulness of both polar angle distribution and spectrum of recoil electrons in testing the TRSV phenomenon. Let us stress that the probed scenarios correspond to the laboratory differential cross section integrated over  $\phi_e$ . We see that this independence of  $\phi_e$  does not eliminate all the interference terms between the standard and exotic  $(S, T, P)_R$  couplings, and in this way there is still the possibility of detecting the TRSV by the precise measurement of these observables. Fig. 7 shows the dependence of  $d\sigma/d\theta_e = (d\sigma/dy)(dy/d\theta_e)$  on  $\theta_e$  for the various scenarios. Upper plot concerns TRSC ( $\theta_{T,R} = \theta_{S,R} = \theta_{P,R} = 0$ ) case, while lower one corresponds to TRSV ( $\theta_{T,R} = \theta_{S,R} =$

$\theta_{P,R} = \pi/2$ ). Fig. 8 displays the same dependence as the Fig. 7, but for the pure contribution from the  $(\hat{\eta}_v)^\perp$ , i. e. when  $\theta_v = \pi/2$ . The significant departure from the standard prediction in the polar angle distribution of recoil electrons for the scenario with  $V-A$  and  $T_R$  interactions can be noticed. For two remaining cases the differences are much smaller. The dashed lines in Fig. 7 correspond to the case of TRSC (upper plot) with  $\theta_e^{max}(T_R) = 34.3^\circ$  and TRSV (lower plot) with  $\theta_e^{max}(T_R) = 33.3^\circ$ , respectively. The similar regularity for the extreme situation with  $\theta_v = \pi/2$  is seen in Fig. 8. Figs. 9, 10 are the plots of  $d\sigma/dy$  as a function of  $y$  depicted with the similar assumptions as for the Figs. 7, 8.

We present the recoil electrons energy spectrum  $d\sigma/dy$  for the scenario with  $V-A$  and  $S_R$  interactions to illustrate the impact of phase of exotic coupling and azimuthal angle of  $(\hat{\eta}_v)^\perp$  on the possibility of TRSV:

$$\left(\frac{d\sigma}{dy}\right)_{V-A,S} = \left(\frac{d\sigma}{dy}\right)_{V-A} + B \left[ |c_S^R|^2 f_S(y) + |c_S^R| \cos(\theta_{S,R} + \phi_v) g_S(y) \right], \quad (3)$$

with the  $y$ -dependent coefficients

$$f_S(y) = 2y \left( \frac{2m_e}{E_v} + y \right) \quad (4)$$

$$g_S(y) = y \left[ -2(c_A^L + c_V^L) + y(c_A^L - c_V^L) \frac{m_e}{E_v} - 4c_A^L \frac{m_e}{E_v} \right].$$

The similar decomposition but with different coefficients  $f$ ,  $g$  holds for the  $V-A$  and  $T_R$ , also  $V-A$  and  $P_R$  interactions. Let us remark that the low energy region of recoil electrons spectrum largely deviates from the standard expectation for the  $V-A$  and  $T_R$  couplings (dashed line in Figs. 9, 10). The cases of  $V-A$  with  $S_R$  and  $V-A$  with  $P_R$  indicate the relatively small deviation for the higher outgoing electrons energy.

#### 5 Conclusions

We have shown that PET may be the useful tool for the detection of the non-standard couplings of RC interacting  $\nu_e$ 's and the effects of TRSV caused by the triple correlations present in the differential cross section for NEES. First, according to the SM prediction the left-right azimuthal asymmetry of the recoil electrons has the maximal value at  $\Phi = \pi/2$  and the location of asymmetry axis is fixed, Figs. 2, 3, 4. If exotic  $(S, T, P)_R$  complex couplings are admitted in NEES on PET, both the magnitude  $A(\Phi_{max})$  and axis  $\Phi_{max}$  of the azimuthal asymmetry may change due to the non-vanishing interferences between the  $V-A$  and  $(S, T, P)_R$  proportional to the TRSC and TRSV correlations, Figs. 5, 6. This departure from the standard prediction is mainly caused by the dependence of azimuthal asymmetry on the azimuthal angle  $\phi_v$  connected with  $(\hat{\eta}_v)^\perp$  as it is shown in the Eq. (2)

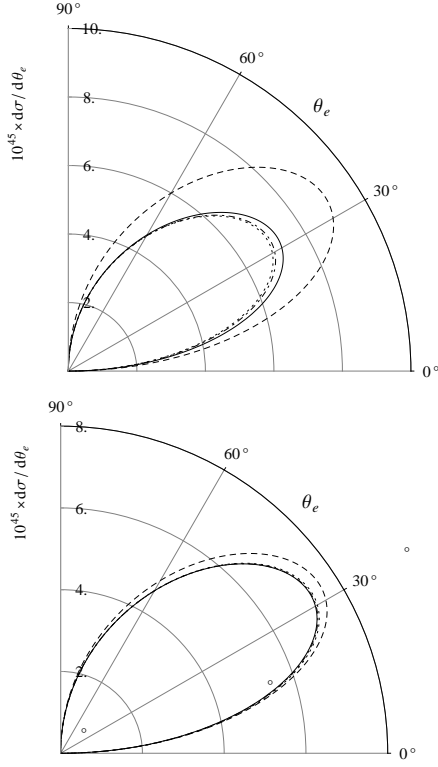


**Fig. 7** Dirac  $\nu_e$ . Plot of  $d\sigma/d\theta_e$  as a function of  $\theta_e$  for  $\hat{\eta}_V \cdot \hat{\mathbf{q}} = -0.95$ ,  $E_V = 1 \text{ MeV}$ . Upper plot for TRSC: standard  $V-A$  interaction (solid line); the combination of  $V-A$  and  $T_R$  when  $|c_T^R| = 0.2$ ,  $\theta_{T,R} = 0$  (dashed line); the case of  $V-A$  and  $S_R$  when  $|c_S^R| = 0.2$ ,  $\theta_{S,R} = 0$  (dotted line);  $V-A$  with  $P_R$  when  $|c_P^R| = 0.2$ ,  $\theta_{P,R} = 0$  (dashed-dotted line). Lower plot for TRSV: standard  $V-A$  interaction (solid line); the combination of  $V-A$  and  $T_R$  when  $|c_T^R| = 0.2$ ,  $\theta_{T,R} = \pi/2$  (dashed line); the case of  $V-A$  and  $S_R$  when  $|c_S^R| = 0.2$ ,  $\theta_{S,R} = \pi/2$  (dotted line);  $V-A$  with  $P_R$  when  $|c_P^R| = 0.2$ ,  $\theta_{P,R} = \pi/2$  (dashed-dotted line).

for the scenario involving  $V-A$  and  $S_R$  couplings. Second, even if the differential cross section is integrated over  $\phi_e$ , but there is PET, the energy spectrum of recoil electrons and the distribution of outgoing electrons polar angle are still sensitive to the interferences, proportional to the angular correlations among  $\hat{\mathbf{q}}, (\hat{\eta}_V)^\perp, (\hat{\eta}_e)^\perp$  vectors, Figs. 7, 8, 9, 10. It is worth pointing out that the measurements of the azimuthal asymmetry and of the polar angle distribution require the intense low-energy  $\nu_e$  sources, the polarized target-electrons, and the detectors observing both the azimuthal angle and polar angle of the scattered electrons with the good angular resolution. The detectors with the very low threshold for the precise measurements of outgoing electrons spectrum would be needed. Let us remind that the ideas of proper detectors such as Hellaz [67–69] and Heron [70–72] have been considered in the literature. The silicon cryogenic detectors (Neganov et al., hep-ex/0105083), the high purity germanium detectors, the semiconductor detectors and the bolometers [73, 74] seem to be also interesting proposals.

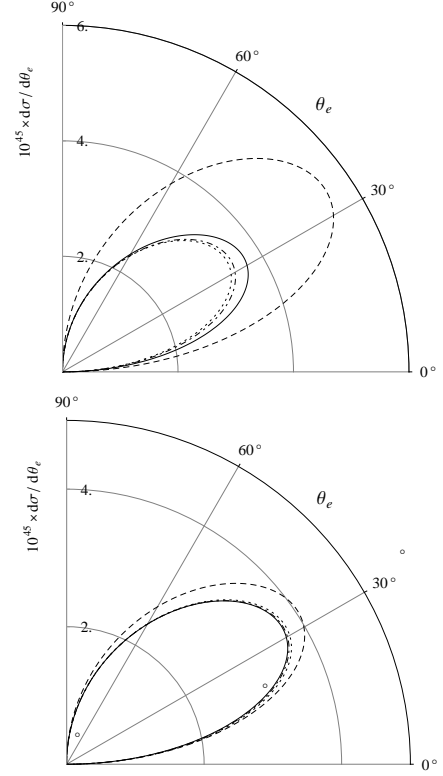


**Fig. 8** Dirac  $\nu_e$ . Plot of  $d\sigma/d\theta_e$  as a function of  $\theta_e$  for  $\theta_V = \pi/2$ ,  $E_V = 1 \text{ MeV}$ . Upper plot for TRSC: standard  $V-A$  interaction (solid line); the combination of  $V-A$  and  $T_R$  when  $|c_T^R| = 0.2$ ,  $\theta_{T,R} = 0$  (dashed line); the case of  $V-A$  and  $S_R$  when  $|c_S^R| = 0.2$ ,  $\theta_{S,R} = 0$  (dotted line);  $V-A$  with  $P_R$  when  $|c_P^R| = 0.2$ ,  $\theta_{P,R} = 0$  (dashed-dotted line). Lower plot for TRSV: standard  $V-A$  interaction (solid line); the combination of  $V-A$  and  $T_R$  when  $|c_T^R| = 0.2$ ,  $\theta_{T,R} = \pi/2$  (dashed line); the case of  $V-A$  and  $S_R$  when  $|c_S^R| = 0.2$ ,  $\theta_{S,R} = \pi/2$  (dotted line);  $V-A$  with  $P_R$  when  $|c_P^R| = 0.2$ ,  $\theta_{P,R} = \pi/2$  (dashed-dotted line).

Our investigation is made in hope to encourage the neutrino laboratories working with the artificial (un)polarized  $\nu$  sources, and to revive the discussion on the feasibility of PET and on the development of ultra-low threshold high-precision detection techniques in the context of TRSV in the low energy leptonic and semileptonic weak interaction processes.

## 6 Appendix 1- General formula on laboratory differential cross section for NEES in PET case

The formula on the laboratory differential cross section calculated with the amplitude  $M_{\nu_e e^-}^D$ , Eq. (1):

$$\begin{aligned} \frac{d^2\sigma}{dyd\phi_e} = & \left( \frac{d^2\sigma}{dyd\phi_e} \right)_{V-A} + \left( \frac{d^2\sigma}{dyd\phi_e} \right)_{V+A} \\ & + \left( \frac{d^2\sigma}{dyd\phi_e} \right)_{(S,T,P)_R} + \left( \frac{d^2\sigma}{dyd\phi_e} \right)_{V-A}^{S_R} \end{aligned} \quad (5)$$

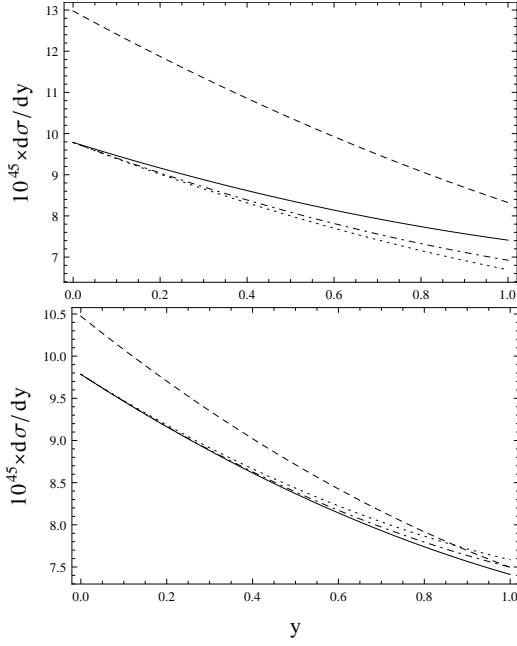


**Fig. 9** Dependence of  $d\sigma/dy$  on  $y$  for  $\hat{\eta}_v \cdot \hat{\mathbf{q}} = -0.95, E_v = 1 \text{ MeV}$ . Upper plot for TRSC: standard  $V-A$  interaction (solid line); the combination of  $V-A$  and  $T_R$  when  $|c_T^R| = 0.2, \theta_{T,R} = 0$  (dashed line); the case of  $V-A$  and  $S_R$  when  $|c_S^R| = 0.2, \theta_{S,R} = 0$  (dotted line);  $V-A$  with  $P_R$  when  $|c_P^R| = 0.2, \theta_{P,R} = 0$  (dashed-dotted line). Lower plot for TRSV: standard  $V-A$  interaction (solid line); the combination of  $V-A$  and  $T_R$  when  $|c_T^R| = 0.2, \theta_{T,R} = \pi/2$  (dashed line); the case of  $V-A$  and  $S_R$  when  $|c_S^R| = 0.2, \theta_{S,R} = \pi/2$  (dotted line);  $V-A$  with  $P_R$  when  $|c_P^R| = 0.2, \theta_{P,R} = \pi/2$  (dashed-dotted line).

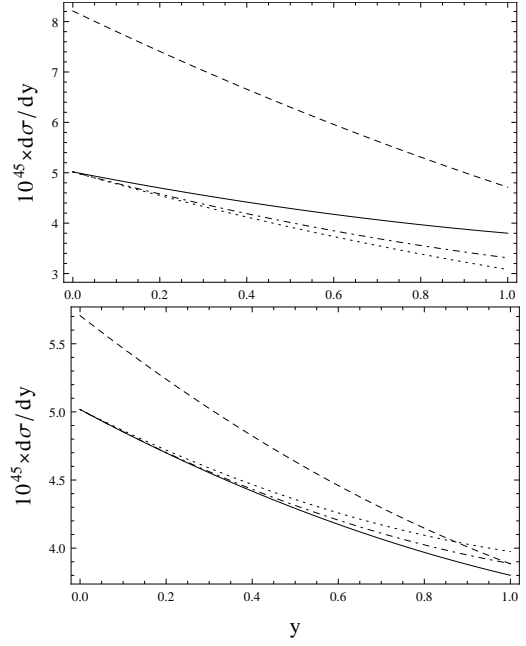


**Fig. 10** Dependence of  $d\sigma/dy$  on  $y$  for  $\theta_v = \pi/2, E_v = 1 \text{ MeV}$ . Upper plot for TRSC: standard  $V-A$  interaction (solid line); the combination of  $V-A$  and  $T_R$  when  $|c_T^R| = 0.2, \theta_{T,R} = 0$  (dashed line); the case of  $V-A$  and  $S_R$  when  $|c_S^R| = 0.2, \theta_{S,R} = 0$  (dotted line);  $V-A$  with  $P_R$  when  $|c_P^R| = 0.2, \theta_{P,R} = 0$  (dashed-dotted line). Lower plot for TRSV: standard  $V-A$  interaction (solid line); the combination of  $V-A$  and  $T_R$  when  $|c_T^R| = 0.2, \theta_{T,R} = \pi/2$  (dashed line); the case of  $V-A$  and  $S_R$  when  $|c_S^R| = 0.2, \theta_{S,R} = \pi/2$  (dotted line);  $V-A$  with  $P_R$  when  $|c_P^R| = 0.2, \theta_{P,R} = \pi/2$  (dashed-dotted line).

$$+ \left( \frac{d^2\sigma}{dyd\phi_e} \right)_{V-A}^{P_R} + \left( \frac{d^2\sigma}{dyd\phi_e} \right)_{V-A}^{T_R} + \left( \frac{d^2\sigma}{dyd\phi_e} \right)_{V+A}^{S_R} \\ + \left( \frac{d^2\sigma}{dyd\phi_e} \right)_{V+A}^{P_R} + \left( \frac{d^2\sigma}{dyd\phi_e} \right)_{V+A}^{T_R},$$

$$\left( \frac{d^2\sigma}{dyd\phi_e} \right)_{V-A} = B(1 - \hat{\eta}_v \cdot \hat{\mathbf{q}}) \left\{ (c_A^L)^2 \left[ (y-2)y + 2 \right. \right. \\ \left. \left. + \frac{m_e}{E_v} y - (\hat{\eta}_e)^\perp \cdot (\hat{\mathbf{p}}_e)^\perp \sqrt{\frac{2m_e}{E_v}} + y(\sqrt{y^3} - 2\sqrt{y}) \right] \right. \\ \left. - (c_V^L)^2 \left[ (\hat{\eta}_e)^\perp \cdot (\hat{\mathbf{p}}_e)^\perp \sqrt{y^3} \sqrt{\frac{2m_e}{E_v}} + y - y^2 \right. \right. \\ \left. \left. + y \left( \frac{m_e}{E_v} + 2 \right) - 2 \right] + 2(c_V^L c_A^L) \left[ (2-y)y \right. \right. \\ \left. \left. + (\hat{\eta}_e)^\perp \cdot (\hat{\mathbf{p}}_e)^\perp (y-1) \sqrt{y \left( \frac{2m_e}{E_v} + y \right)} \right] \right\},$$

$$\left( \frac{d^2\sigma}{dyd\phi_e} \right)_{V+A} = B(1 + \hat{\eta}_v \cdot \hat{\mathbf{q}}) \left\{ (c_A^R)^2 \left[ (y-2)y + 2 \right. \right. \\ \left. \left. + \frac{m_e}{E_v} y + (\hat{\eta}_e)^\perp \cdot (\hat{\mathbf{p}}_e)^\perp \sqrt{\frac{2m_e}{E_v}} + y(\sqrt{y^3} - 2\sqrt{y}) \right] \right. \\ \left. + (c_V^R)^2 \left[ (\hat{\eta}_e)^\perp \cdot (\hat{\mathbf{p}}_e)^\perp \sqrt{y^3} \sqrt{\frac{2m_e}{E_v}} + y + y^2 \right. \right. \\ \left. \left. - y \left( \frac{m_e}{E_v} + 2 \right) + 2 \right] + 2(c_V^R c_A^R) \left[ (2-y)y \right. \right. \\ \left. \left. + (\hat{\eta}_e)^\perp \cdot (\hat{\mathbf{p}}_e)^\perp (1-y) \sqrt{y \left( \frac{2m_e}{E_v} + y \right)} \right] \right\},$$

$$\left( \frac{d^2\sigma}{dyd\phi_e} \right)_{(S,T,P)_R} = B \left\{ y \left( y + 2 \frac{m_e}{E_v} \right) |c_S^R|^2 + y^2 |c_P^R|^2 \right. \quad (8)$$

$$+ 2 \left[ \left( (2-y)^2 - \frac{m_e}{E_v} y - (\hat{\eta}_e)^\perp \cdot (\hat{\mathbf{p}}_e)^\perp \hat{\eta}_v \cdot \hat{\mathbf{q}} \sqrt{\frac{2m_e}{E_v}} + y \right. \right. \\ \left. \left. \cdot (\sqrt{y^3} - 2\sqrt{y}) \right) |c_T^R|^2 + y \left( (y-2) \right. \right. \\ \left. \left. - (\hat{\eta}_e)^\perp \cdot (\hat{\mathbf{p}}_e)^\perp \hat{\eta}_v \cdot \hat{\mathbf{q}} \sqrt{\left( \frac{2m_e}{E_v} + y \right) y} \right) \text{Re}(c_P^R c_T^{*R}) \right. \\ \left. - (\hat{\eta}_e)^\perp \cdot (\hat{\mathbf{p}}_e)^\perp \hat{\eta}_v \cdot \hat{\mathbf{q}} \sqrt{\frac{2m_e}{E_v}} + y \sqrt{y^3} \text{Re}(c_S^R c_P^{*R}) \right. \\ \left. + (y-2) \left( y - (\hat{\eta}_e)^\perp \cdot (\hat{\mathbf{p}}_e)^\perp \hat{\eta}_v \cdot \hat{\mathbf{q}} \sqrt{y \left( \frac{2m_e}{E_v} + y \right)} \right) \right. \\ \left. \cdot \text{Re}(c_S^R c_T^{*R}) + 2 \sqrt{y \left( y + 2 \frac{m_e}{E_v} \right)} (\hat{\eta}_e)^\perp \cdot (\hat{\mathbf{q}} \times (\hat{\mathbf{p}}_e)^\perp) \right\},$$



$$\begin{aligned}
& + y(\hat{\mathbf{p}}_e)^\perp \cdot ((\hat{\boldsymbol{\eta}}_e)^\perp \times (\hat{\boldsymbol{\eta}}_v)^\perp) \text{Im}(c_S^R) \\
& + y(y-2)(\hat{\boldsymbol{\eta}}_e)^\perp \cdot (\hat{\boldsymbol{\eta}}_v)^\perp \text{Re}(c_S^R) \\
& + \left( \frac{E_v}{m_e} y^2 + 2y \right) (\hat{\boldsymbol{\eta}}_v)^\perp \cdot (\hat{\mathbf{p}}_e)^\perp \left( (\hat{\boldsymbol{\eta}}_e)^\perp \cdot (\hat{\mathbf{p}}_e)^\perp \text{Re}(c_S^R) \right. \\
& \left. - (\hat{\boldsymbol{\eta}}_e)^\perp \cdot (\hat{\mathbf{q}} \times (\hat{\mathbf{p}}_e)^\perp) \text{Im}(c_S^R) \right) \Bigg] \Bigg\},
\end{aligned}$$

$$\left( \frac{d^2 \sigma}{dy d\phi_e} \right)_{v+A}^{Pr} = B \left\{ c_V^R \frac{E_v}{m_e} \left[ y \sqrt{y \left( \frac{2m_e}{E_v} + y \right)} \right. \right. \quad (13)$$

$$\begin{aligned}
& \cdot \left( (\hat{\mathbf{p}}_e)^\perp \cdot ((\hat{\boldsymbol{\eta}}_e)^\perp \times (\hat{\boldsymbol{\eta}}_v)^\perp) \text{Im}(c_P^R) \right) + \left( y^2 + \frac{2m_e y}{E_v} \right) \\
& \cdot \left( (\hat{\boldsymbol{\eta}}_e)^\perp \cdot (\hat{\mathbf{p}}_e)^\perp \left( -(\hat{\boldsymbol{\eta}}_v)^\perp \cdot (\hat{\mathbf{p}}_e)^\perp \text{Re}(c_P^R) \right. \right. \\
& \left. \left. + (\hat{\boldsymbol{\eta}}_v)^\perp \cdot (\hat{\mathbf{q}} \times (\hat{\mathbf{p}}_e)^\perp) \text{Im}(c_P^R) \right) \right) - \left( \hat{\mathbf{q}} \cdot ((\hat{\boldsymbol{\eta}}_e)^\perp \times (\hat{\boldsymbol{\eta}}_v)^\perp) \right. \\
& \left. \cdot \text{Im}(c_P^R) + \frac{m_e}{E_v} (\hat{\boldsymbol{\eta}}_e)^\perp \cdot (\hat{\boldsymbol{\eta}}_v)^\perp \text{Re}(c_P^R) \right) y^2 \Bigg] \\
& + c_A^R \left[ y \sqrt{\left( \frac{2m_e}{E_v} + y \right)} y (\hat{\mathbf{p}}_e)^\perp \cdot ((\hat{\boldsymbol{\eta}}_e)^\perp \times (\hat{\boldsymbol{\eta}}_v)^\perp) \right. \\
& \cdot \text{Im}(c_P^R) + y(y-2)(\hat{\boldsymbol{\eta}}_e)^\perp \cdot (\hat{\boldsymbol{\eta}}_v)^\perp \text{Re}(c_P^R) \\
& + \left( \frac{E_v}{m_e} y^2 + 2y \right) (\hat{\boldsymbol{\eta}}_v)^\perp \cdot (\hat{\mathbf{p}}_e)^\perp \left( (\hat{\boldsymbol{\eta}}_e)^\perp \cdot (\hat{\mathbf{p}}_e)^\perp \text{Re}(c_P^R) \right. \\
& \left. - (\hat{\boldsymbol{\eta}}_e)^\perp \cdot (\hat{\mathbf{q}} \times (\hat{\mathbf{p}}_e)^\perp) \text{Im}(c_P^R) \right) \Bigg] \Bigg\},
\end{aligned}$$

$$\left( \frac{d^2 \sigma}{dy d\phi_e} \right)_{v+A}^{Tr} = 2B \left\{ \frac{E_v}{m_e} \left[ c_A^R \left( \sqrt{y \left( \frac{2m_e}{E_v} + y \right)} \right) \right. \right. \quad (14)$$

$$\begin{aligned}
& \cdot \left( 1 - 2y + \frac{2m_e y}{E_v} \right) (\hat{\mathbf{p}}_e)^\perp \cdot ((\hat{\boldsymbol{\eta}}_e)^\perp \times (\hat{\boldsymbol{\eta}}_v)^\perp) \text{Im}(c_T^R) \\
& + 2 \left( y^2 + \frac{2m_e y}{E_v} \right) \left( (\hat{\boldsymbol{\eta}}_v)^\perp \cdot (\hat{\mathbf{p}}_e)^\perp (\hat{\boldsymbol{\eta}}_e)^\perp \cdot (\hat{\mathbf{q}} \times (\hat{\mathbf{p}}_e)^\perp) \right. \\
& \left. - (\hat{\boldsymbol{\eta}}_e)^\perp \cdot (\hat{\mathbf{p}}_e)^\perp (\hat{\boldsymbol{\eta}}_v)^\perp \cdot (\hat{\mathbf{q}} \times (\hat{\mathbf{p}}_e)^\perp) \right) \text{Im}(c_T^R) \\
& + (2y-1) \left( y + \frac{2m_e}{E_v} \right) \hat{\mathbf{q}} \cdot ((\hat{\boldsymbol{\eta}}_e)^\perp \times (\hat{\boldsymbol{\eta}}_v)^\perp) \text{Im}(c_T^R) \\
& - \left( \frac{m_e}{E_v} \right) (y-2)(\hat{\boldsymbol{\eta}}_e)^\perp \cdot (\hat{\boldsymbol{\eta}}_v)^\perp \text{Re}(c_T^R) \\
& + \left( \frac{m_e}{E_v} \right) \sqrt{y \left( \frac{2m_e}{E_v} + y \right)} \left( -(\hat{\boldsymbol{\eta}}_v)^\perp \cdot (\hat{\mathbf{p}}_e)^\perp \text{Re}(c_T^R) \right. \\
& \left. + (\hat{\boldsymbol{\eta}}_v)^\perp \cdot (\hat{\mathbf{q}} \times (\hat{\mathbf{p}}_e)^\perp) \text{Im}(c_T^R) \right) \Bigg) \Bigg\}
\end{aligned}$$

$$+ c_V^R \left( \left( 2(1-y) + \left( \frac{m_e}{E_v} \right) (1-2y) \right) \sqrt{\left( \frac{2m_e}{E_v} + y \right)} y \right.$$

$$\begin{aligned}
& \cdot \left( (\hat{\mathbf{p}}_e)^\perp \cdot ((\hat{\boldsymbol{\eta}}_e)^\perp \times (\hat{\boldsymbol{\eta}}_v)^\perp) \text{Im}(c_T^R) \right) + 2 \left( y^2 + \frac{2m_e y}{E_v} \right) \\
& \cdot \left( (\hat{\boldsymbol{\eta}}_v)^\perp \cdot (\hat{\mathbf{p}}_e)^\perp (\hat{\boldsymbol{\eta}}_e)^\perp \cdot (\hat{\mathbf{q}} \times (\hat{\mathbf{p}}_e)^\perp) \right. \\
& \left. - (\hat{\boldsymbol{\eta}}_e)^\perp \cdot (\hat{\mathbf{p}}_e)^\perp (\hat{\boldsymbol{\eta}}_v)^\perp \cdot (\hat{\mathbf{q}} \times (\hat{\mathbf{p}}_e)^\perp) \right) \text{Im}(c_T^R) \\
& + 2(y-1) \left( y + \frac{m_e}{E_v} \right) \hat{\mathbf{q}} \cdot ((\hat{\boldsymbol{\eta}}_e)^\perp \times (\hat{\boldsymbol{\eta}}_v)^\perp) \text{Im}(c_T^R) \Bigg] \\
& + \left( 2-y + \frac{m_e y}{E_v} \right) (\hat{\boldsymbol{\eta}}_e)^\perp \cdot (\hat{\boldsymbol{\eta}}_v)^\perp \text{Re}(c_T^R) \Bigg) \Bigg\}.
\end{aligned}$$

$$y \equiv \frac{T_e}{E_v} = \frac{m_e}{E_v} \frac{2 \cos^2 \theta_e}{(1 + \frac{m_e}{E_v})^2 - \cos^2 \theta_e} \quad (15)$$

is the ratio of the kinetic energy of the recoil electron  $T_e$  to the incoming  $v_e$  energy  $E_v$ .  $m_e$  is the electron mass;  $B \equiv (E_v m_e / 4\pi^2) (G_F^2 / 2)$ .  $\hat{\boldsymbol{\eta}}_v$  is the unit 3-vector of  $v_e$  spin polarization in its rest frame.  $(\hat{\boldsymbol{\eta}}_v \cdot \hat{\mathbf{q}}) \hat{\mathbf{q}}$  is the longitudinal component of  $v_e$  spin polarization.  $|\hat{\boldsymbol{\eta}}_v \cdot \hat{\mathbf{q}}| = |1 - 2Q_L^Y|$ , where  $Q_L^Y$  is the probability of producing the LC  $v_e$ .

## 7 Appendix 2 - Definitions of the asymmetry functions

The asymmetry function  $A(\Phi)$  is defined as

$$A(\Phi) := \frac{\int_{\Phi}^{\Phi+\pi} \frac{d\sigma}{d\phi_e} d\phi_e - \int_{\Phi+\pi}^{\Phi+2\pi} \frac{d\sigma}{d\phi_e} d\phi_e}{\int_{\Phi}^{\Phi+\pi} \frac{d\sigma}{d\phi_e} d\phi_e + \int_{\Phi+\pi}^{\Phi+2\pi} \frac{d\sigma}{d\phi_e} d\phi_e}. \quad (16)$$

Two other asymmetry functions are employed:

$$A_y(\Phi) := \frac{\int_{\Phi}^{\Phi+\pi} \frac{d^2 \sigma}{d\phi_e dy} d\phi_e - \int_{\Phi+\pi}^{\Phi+2\pi} \frac{d^2 \sigma}{d\phi_e dy} d\phi_e}{\int_{\Phi}^{\Phi+\pi} \frac{d^2 \sigma}{d\phi_e dy} d\phi_e + \int_{\Phi+\pi}^{\Phi+2\pi} \frac{d^2 \sigma}{d\phi_e dy} d\phi_e}, \quad (17)$$

$$A_{\theta_e}(\Phi) := \frac{\int_{\Phi}^{\Phi+\pi} \frac{d^2 \sigma}{d\phi_e d\theta_e} d\phi_e - \int_{\Phi+\pi}^{\Phi+2\pi} \frac{d^2 \sigma}{d\phi_e d\theta_e} d\phi_e}{\int_{\Phi}^{\Phi+\pi} \frac{d^2 \sigma}{d\phi_e d\theta_e} d\phi_e + \int_{\Phi+\pi}^{\Phi+2\pi} \frac{d^2 \sigma}{d\phi_e d\theta_e} d\phi_e}. \quad (18)$$

## References

1. S. L. Glashow, Nucl. Phys. **22**, 579 (1961)
2. S. Weinberg, Phys. Rev. Lett. **19**, 1264 (1967)
3. A. Salam, A. Salam, in *Elementary Particle Theory* (Almqvist and Wiksells, Stockholm, 1969)
4. R. P. Feynman, M. Gell-Mann, Phys. Rev. **109**, 193 (1958)
5. E. C. G. Sudarshan, R. E. Marshak, Phys. Rev. **109**, 1860 (1958)

6. J.H. Christenson, J.W. Cronin, V.L. Fitch and R. Turlay, *Phys. Rev. Lett.* **13**, 138 (1964)
7. B. Aubert et al., *Phys. Rev. Lett.* **87**, 091801 (2001)
8. K. Abe et al., *Phys. Rev. Lett.* **87**, 091802 (2001)
9. M. Kobayashi, T. Maskawa, *Prog. Theor. Phys.* **49**, 652 (1973)
10. A. Riotto, M. Trodden, *Annu. Rev. Nucl. Part. Sci.* **49**, 35 (1999)
11. J.C. Pati, A. Salam, *Phys. Rev. D* **10**, 275 (1974)
12. R. Mohapatra, J.C. Pati, *Phys. Rev. D* **11**, 566 (1975); *Phys. Rev. D* **11**, 558 (1975)
13. R.N. Mohapatra, G. Senjanovic, *Phys. Rev. D* **12**, 1502 (1975); *Phys. Rev. D* **23**, 165 (1981)
14. M. A. B. Beg et al., *Phys. Rev. Lett.* **38**, 1252 (1977)
15. P. Herczeg, *Phys. Rev. D* **34**, 3449 (1986)
16. A. Jodidio et al., *Phys. Rev. D* **34**, 1967 (1986)
17. E. J. Eichten, K. D. Lane, M.E. Peskin, *Phys. Rev. Lett.* **50**, 811 (1983)
18. P. Herczeg, *Prog. Part. Nucl. Phys.* **46**, 413 (2001)
19. N. Arkani-Hamed, S. Dimopoulos, G. Dvali, J. March-Russell, *Phys. Lett. B* **429**, 263 (1998).
20. T. Banks, A. Zaks, *Nucl. Phys. B* **196**, 189 (1982)
21. H. Georgi, *Phys. Rev. Lett.* **98**, 221601 (2007)
22. H. Georgi, *Phys. Lett. B* **650**, 275 (2007)
23. K. Cheung, W.Y. Keung, T.C. Yuan, *Phys. Rev. Lett* **99**, 051803 (2007)
24. K. Cheung, W.Y. Keung, T.C. Yuan, *Phys. Rev. D* **76**, 055003 (2007)
25. S. L. Chen, X. G. He, *Phys. Rev. D* **76**, 091702 (2007)
26. A. B. Balantekin, K. O. Ozansoy, *Phys. Rev. D* **76**, 095014 (2007)
27. J. Barranco et al., *Phys. Rev. D* **79**, 073011 (2009)
28. D. Montanino, M. Picariello, J. Pulido, *Phys. Rev. D* **77**, 093011 (2008)
29. S. Zhou, *Phys. Lett. B* **659**, 336 (2008)
30. B. Grinstein, K. A. Intriligator, I. Z. Rothstein, *Phys. Lett. B* **662**, 367 (2008)
31. M. Deniz et al., *Phys. Rev. D* **82**, 033004 (2010)
32. J. Barranco et al., *Int. J. Mod. Phys. A* **27**, 1250147 (2012)
33. S. Geer, *Phys. Rev. D* **57**, 6989 (1998)
34. S. Geer, *Phys. Rev. D* **59**, 039903 (1999)
35. L. J. Lising et al., *Phys. Rev. C* **62**, 055501 (2000)
36. P. Herczeg, *J. Res. Natl. Inst. Stand. Technol.* **110**, 453 (2005)
37. R. Huber et al., *Phys. Rev. Lett.* **90**, 202301 (2003)
38. K. Bodek et al., *J. Res. Natl. Inst. Stand. Technol.* **110**, 461 (2005)
39. H. P. Mumm et al., *Phys. Rev. Lett.* **107**, 102301 (2011)
40. S. Weinberg, *Phys. Rev. D* **42**, 860 (1990)
41. R. Garisto, G. L. Kane, *Phys. Rev. D* **44**, 2038 (1991)
42. G. Belanger, C. Q. Geng, *Phys. Rev. D* **44**, 2789 (1991)
43. G. H. Wu, J. N. Ng, *Phys. Lett. B* **392**, 93 (1997)
44. E. Gabrielli, *Phys. Lett. B* **301**, 409 (1993)
45. B. Babussinov et al., *Nucl. Instrum. and Meth. A* **694**, 335 (2012)
46. M. Misiaszek et al., *Nucl. Phys. B* **734**, 203 (2006)
47. J. Bernabeu et al., *Phys. Lett. B* **613**, 162 (2005)
48. V. A. Guseinov et al., *Phys. Rev. D* **75**, 073021 (2007)
49. S. Ciechanowicz et al., *Phys. Rev. D* **71**, 093006 (2005)
50. P. Minkowski, M. Passera, *Phys. Lett. B* **541**, 151 (2002)
51. T. I. Rashba, V. B. Semikoz, *Phys. Lett. B* **479**, 218 (2000)
52. W.-T. Ni et al., *Phys. Rev. Lett.* **82**, 2439 (1999)
53. W. Bialek et al., *Phys. Rev. Lett.* **56**, 1623 (1986)
54. P. V. Vorobyov, Y. I. Gitarts, *Phys. Lett. B* **208**, 146 (1988)
55. K.A. Olive et al. (Particle Data Group), *Chin. Phys. C* **38**, 090001 (2014)
56. G. Bellini et al., *JHEP* **08**, 038 (2013)
57. C. Athanassopoulos et al., *Phys. Rev. Lett.* **75**, 2650 (1995)
58. C. Athanassopoulos et al., *Phys. Rev. C* **54**, 2685 (1996)
59. A. Aguilar et al., *Phys. Rev. D* **64**, 112007 (2001)
60. A. Anguilar-Arevalo et al., *Phys. Rev. Lett.* **105**, 181801 (2010)
61. Th. Mueller et al., *Phys. Rev. C* **83**, 054615 (2011)
62. P. Huber, *Phys. Rev. C* **84**, 024617 (2011)
63. G. Mention et al., *Phys. Rev. D* **83**, 073006 (2011)
64. S. Ciechanowicz, M. Misiaszek, S. Sobków, *Eur. Phys. J. C* **32**, s01, s151 (2003)
65. D. M. Webber et al., *Phys. Rev. Lett.* **106**, 041803 (2011)
66. L. Michel, A. S. Wightman, *Phys. Rev.* **98**, 1190 (1955)
67. F. Arzarello et al., Report No. CERN-LAA/94-19, College de France LPC/94-28, 1994
68. J. Seguinot et al., Report No. LPC 95 08, College de France, Laboratoire de Physique Corpusculaire, 1995
69. A. Sarrat, *Nucl. Phys. Proc. Suppl.* **95**, 177 (2001)
70. R. E. Lanou et al., The Heron project. Abstracts of Papers of the American Chemical Society 2(217), 021-NUCL 1999
71. Y.H. Huang, R. E. Lanou, H. J. Maris, G. M. Seidel, B. Sethumadhavan, W. Yao, *Astropart. Phys.* **30**, 1 (2008)
72. J. S. Adams, Y. H. Huang, Y. H. Kim, R. E. Lanou, H. J. Maris, G. M. Seidel, The HERON project, chapter 8, pages 70-80, 2002
73. C. E. Aalseth et al., *Phys. Rev. Lett.* **106**, 131301 (2011)
74. C. Enss, *Cryogenic Particle Detection* (Springer-Verlag Berlin Heidelberg, 2005)

